Numerical investigation of slamming loads on floating offshore wind turbines

Marc Batlle Martin, Jeffrey Harris, Paul Renaud, Florian Hulin, Jean-François Filipot

Numerical investigation of slamming loads on floating offshore wind turbines

Marc Batlle Martin[1,2]*, Jeffrey C. Harris*[2]*, Paul Renaud*[1]*, Florian Hulin*[1] *and Jean-François Filipot*[1]
[1] France Energies Marines, Plouzané, France
[2] LHSV, Ecole des Ponts, Cerema, EDF R&D, Chatou, France

ABSTRACT

This paper presents the results of ongoing work regarding numerical simulations of breaking wave impacts on a surface-piercing cylinder. The computational fluid dynamics solver, *Code_Saturne*, using the volume of fluid approach, is presented and utilised for offshore hydrodynamics. Phase-focused waves are employed to recreate singular breaking events under relatively controlled conditions. The fluid shape and kinematics are described during the breaking process and the load produced by a plunging breaker on a rigid cylinder is investigated.

KEY WORDS: ESBW; slamming; focused waves; VOF; numerical wave tank; CFD.

INTRODUCTION

Bottom fixed and floating offshore wind turbines are growing in popularity and developing towards being an economically viable alternative to conventional carbon-based energy forms. During the past few decades, most offshore wind turbines were installed on monopile foundations relatively close to the coastline. More recently, the energy sector is gradually embracing the possibility of expanding towards deeper waters, mostly motivated by the presence of stronger and more stable winds, and the availability of a wider range of areas. The water depths on these locations make the installation of conventional bottom fixed structures difficult, and newer approaches using floating turbines are more viable solutions.

The rapid growth of this sector and the large number of turbines to be installed in a single park requires different approaches for their design, manufacturing, and installation, compared to the typical procedure for existing offshore structures, e.g., oil and gas. These new approaches provide an opportunity for optimization and standardization, however, and old design challenges, which may carry general uncertainties, need to be revisited and properly addressed.

The targeted locations for offshore wind turbines are often affected by the presence of energetic steep or breaking waves (ESBWs) and these may be an important contributor to the overall loading of the structure affecting the Ultimate Limit State. Unlike nonbreaking focused waves (e.g., Sriram et al., 2020), when ESBWs interact with the structures, they lead to violent motions of the liquid and a significant transfer of momentum occurs in very localised spatial and temporal scales. These so-called *slamming events*, are likely to occur during storm conditions and the related resultant forces are poorly predicted if using the classic Morison's formula (Morison et al., 1950). The applicability of such an approach in complex situations has been studied by Saincher et al. (2022).

In terms of input waves, although it begins to be feasible to consider large-scale simulations of irregular sea-states, such as Pierella et al. (2020), it is often more useful to consider focused waves. In a focused wave packet, dispersion of deep-water waves is used to generate a single breaking wave group, which has an advantage for easily reproducing and studying unsteady breaking waves. This also allows a significant reduction of the duration and the complexity in the simulations related to sea states, which permits a balance of accuracy and computational costs from the numerical simulations point of view. Many different spectra of focused waves have been considered for studies before; a realistic waveform can be produced using NewWave theory, as described by Tromans et al. (1991). Incidentally, while modeling the propagation of these waves is physically well understood, it can be important to validate numerical models anyway, as Vyzikas et al. (2021) found that different models can give moderately different results for certain harmonics of a wave group, likely due to the large steepness. Focused waves for floating structures have previously been used for blind comparative studies as a result, using NewWave theory, as described by Ransley et al. (2020).

For theories of slamming, the original works of von Kármán (1929) and Wagner (1932) investigated the water entry of a rigid object on a flat surface fluid, mimicking the impact pressures on seaplanes during landing. The theory of Wagner included the pile-up effect and the full effect of the added mass, as an extension to the work of von Kármán. Goda et al. (1966) extended this work for water waves, introducing the concept of the curling factor, λ, which indicates the height of the impact area as a function of the incident wave height. In recent years, Wienke and Oumeraci (2005) further investigated experimentally the slamming load exerted by phase-focused breaking waves on an inclined slender cylinder. During the JIP-WiFi project (Paulsen et al., 2019), these existing formulas were revisited and the project resulted in an

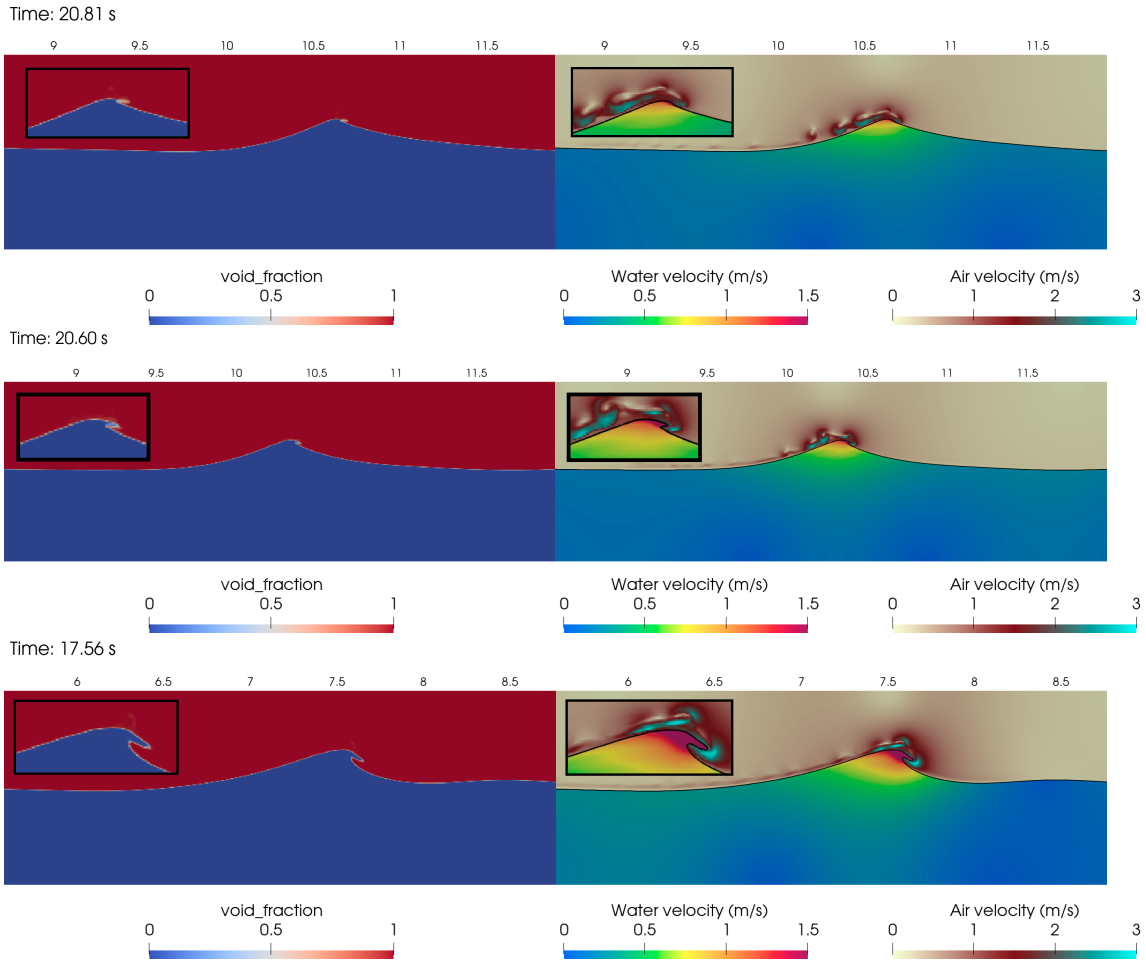

Fig. 1 VOF and velocity field for the weak-spilling A3 (top), spilling A4 (mid) and strong plunging A6 (bottom) breaking 2D focused packets.

expression based on empirical fitting over a large number of slamming impacts produced by multiple irregular sea-states related to shallow to intermediate water depths. The particular interest in further CFD results here are to improve engineering models, however, as even for a fixed structure, Veic and Suilisz (2018) notably found that the Wienke's model (Wienke and Oumeraci, 2005), often cited, such as by the IEC design standard sometimes did not predict the forces accurately.

The work presented in the paper is part of the DIMPACT project (Design of floating wind turbines and impacts of energetic steep and breaking waves) which benefits from the previous experience acquired during the DiMe project (Filipot et al., 2019). The objectives are to reduce the uncertainties related to slamming loads exerted by ESBW on floating offshore wind turbines by analysing experimentally and numerically this phenomenon in deep and intermediate water conditions. The present work analyses the first numerical results obtained of slamming phase-focused waves on a fixed cylinder.

This article is organized as follows: in Section 2, the governing equations and numerical implementation of the method is introduced; Section 3 presents the ability of the solver employed to simulate different wave breaking situations using a 2D numerical wave tank (NWT); in Section 4, a description of the results obtained during a 3D computation of a plunging impact on a cylinder is presented and the final section is the discussion and conclusions.

NUMERICAL THEORY

The solver employed for the present work is part of the open-source *Code_Saturne* model (Archambeau et al., 2004) developed by EDF R&D. This is a Navier-Stokes model which is able to resolve free-surface motion with multiple approaches, including a moving mesh (arbitrary Lagrangian-Eulerian or ALE) scheme (Ferrand and Harris, 2021). For the present application, in order to be able to capture the dyanmics of a breaking wave, the volume of fluid (VOF) approach. Specifically, this is based on a version of the M-CICSAM advection scheme (Zhang et al., 2014) for algebraic VOF.

The incompressible Navier-Stokes equations are used to describe viscous fluid dynamics. For a fluid without other external forces than gravity, the equation for continuity and momentum can be written as:

$$\partial_t(\rho\overline{u}) + \nabla\cdot(\overline{u}\otimes\rho\overline{u}) = -\nabla p + \nabla\cdot\underline{\tau}(\overline{u}) + (\rho-\rho_{void})\overline{g}\,,$$
$$\nabla\cdot\overline{u} = 0\,,$$
$$\partial_t\alpha + \nabla\cdot(\alpha\overline{u}) = 0\,,$$

with ρ the fluid density, $\overline{u}$ the velocity, p the pressure and $\underline{\tau}$ the stress tensor. No turbulence model is used in the present work as it is assumed to be negligible for the propagation and the initial instants of the wave overturning and impact. The scalar field α is used in the VOF method, defined as the volume fraction of one of the two phases. In what follows, these two phases will be air and water. The fluid fraction (or void

fraction) is:

$$\alpha = \frac{\text{void/air volume in a cell}}{\text{volume of the cell}}$$

The fluid properties for a cell are therefore a linear combination of the density and viscosity of air, as a function of α (i.e. $\rho = \rho_{air}\alpha + \rho_{water}(1-\alpha)$).

Wave generation

Waves are generated through boundary conditions that provide the velocity field, as well as the VOF field α, according to the selected wave theory. As an approximation, the velocity in the air phase can be taken to be zero. For the water phase, we take a velocity field corresponding to linear wave theory for a given wave elevation signal (Dean and Dalrymple, 1991), but this could be replaced with higher-order wave theories (e.g., Sriram et al., 2015), the results from another model for important events, similar to the database of fully nonlinear wave kinematics produced by Pierella et al. (2020), or directly a coupled model could be used, such as by Corte and Grilli (2006).

The present work makes use of phase-focused waves to simulate a chosen ESBW that could represent an extreme wave within an irregular sea state. The wave packets are generated at the NWT upstream boundary with a superposition of N sinusoidal components of steepness $a_n k_n$ according to the linear wave theory, as follows (Rapp et al., 1990):

$$\eta(0,z,t) = \sum_{n=1}^{N} a_n cos\left[2\pi f_n(t-t_f) + k_n x_f\right].$$

The wave packet global steepness S is chosen to be constant for each configuration and the waves amplitudes are calculated as $a_n = S/(Nk_n)$. The discrete frequencies f_n are uniformly spaced over the band $\Delta f = f_N - f_1$ with a central frequency defined by $f_c = 1/2(f_N + f_1)$. The terms x_f and t_f are the predefined linear theory estimates of the location and time of the focal point respectively.

2D WAVE PACKET

In this section, phase-focused waves are considered in a two-dimensional (2D) domain to investigate the wave breaking process. The NWT is modelled using a non-conformal rectangular mesh with a refined region (cell length $\Delta x = \Delta z = 5$ mm) around the free surface location, and larger cells, with cell sizes twice larger in each direction, within the air and water region. The boundary conditions are selected as an inlet wave generation with prescribed velocities and void fractions, as described in the previous section. The top boundary is selected as an open boundary with an imposed pressure and the bottom is defined as a smooth wall. On the right side of the domain, the outlet is defined as symmetric plane; reflection is possible from this boundary, but it is not expected to affect the structure before the targeted breaking event occurs. Finally, the time steps are selected to be constants and small enough to maintain the maximum Courant-Friedrichs-Lewy number (CFL) below 1. Hereafter, the location x_f and time t_f of the focal point are 9 m and 20 s.

In Table 1, the wave packet input parameters are summarized for the three studied configurations. These are chosen to match the work presented by Derakhti et al. (2018) in order to facilitate some inter-model comparisons below. The only difference between each of the three chosen cases (A3, A4, and A6) is the wave packet global steepness. In Fig. 1, the void fraction and the velocity fields obtained with *Code_Saturne* are presented for the three cases near the moment of wave breaking. Using these wave inputs, the wave breaking go from a weak-spilling situation, case A3, to a strong plunging breaker, case A6.

Table 1 Parameters for constant-steepness wave packets, from spilling to plunging conditions.

Case	S	f_c (s^{-1})	$\Delta f/f_c$	N	h (m)
A3	0.302	0.88	0.75	32	0.6
A4	0.31	0.88	0.75	32	0.6
A6	0.44	0.88	0.75	32	0.6

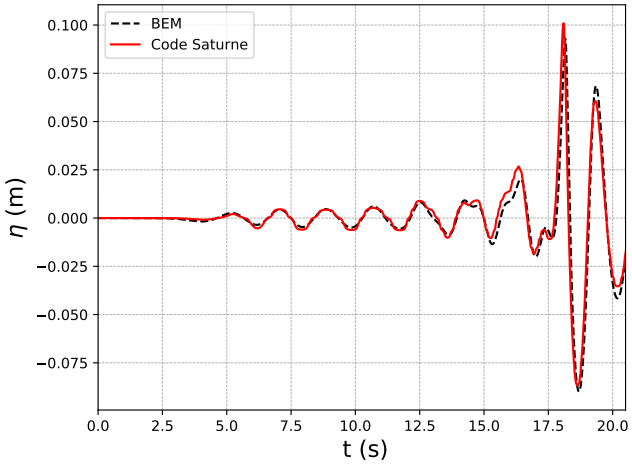

Fig. 2 Comparison between a potential flow solution using the model of Grilli et al. (1989) and *Code_Saturne* for the A4 test case of Derakhti et al. (2018), at a point 8 m from the wavemaker boundary (therefore before the breaking point)

In each case, the wave breaking appears to be resolved by capturing the crest overturning. By looking at the void fraction field, one can see how the interface is overall well preserved and sharp, represented only by one cell in the vertical direction. The smaller wave overturning tip is more diffuse compared to the strong plunging, with several cells with void fraction values around 0.5. The diffusion of the interface may be problematic when investigating a wave impact as it reduces the water density and, thus, the momentum. Regarding the velocity fields, the higher velocities within the liquid region are located at the wave crest and the overturning tip. The velocity field on the air region presents the drag phenomenon of the wave crest and how the air escapes upstream from the overturning enclosing. This seems to pull a portion of the water fraction in front of the overturning tip (see the void fraction field). The velocity field presents a smooth transition over the sudden jump between the refined and non-refined mesh regions.

Proceeding into a preliminary validation of the model, in particular to see if the model setup is able to avoid issues of numerical dissipation, the fully non-linear potential flow (FNPF) solver of Grilli et al. (1989, 1996), based on the boundary element method, is used to reproduce a similar wave input (based on a flap wavemaker motion and assuming linear theory at the wavemaker boundary) as the spilling breaker, case A4. This model solves the Laplace equation for the velocity potential, based on Green's second identity, transformed into a Boundary Integral Equation expressed over the domain boundary Γ, at a set of collocation points $\mathbf{x}_i$ ($i = 1, \ldots, N_\Gamma$),

$$\alpha(\mathbf{x}_i)\phi(\mathbf{x}_i) = \int_\Gamma \left[\frac{\partial \phi}{\partial n}(\mathbf{x})G(\mathbf{x}-\mathbf{x}_i) - \phi(\mathbf{x})\frac{\partial G}{\partial n}(\mathbf{x}-\mathbf{x}_i)\right] d\Gamma,$$

with α the interior solid angle made by the boundary at $\mathbf{x}_i$ (e.g., for

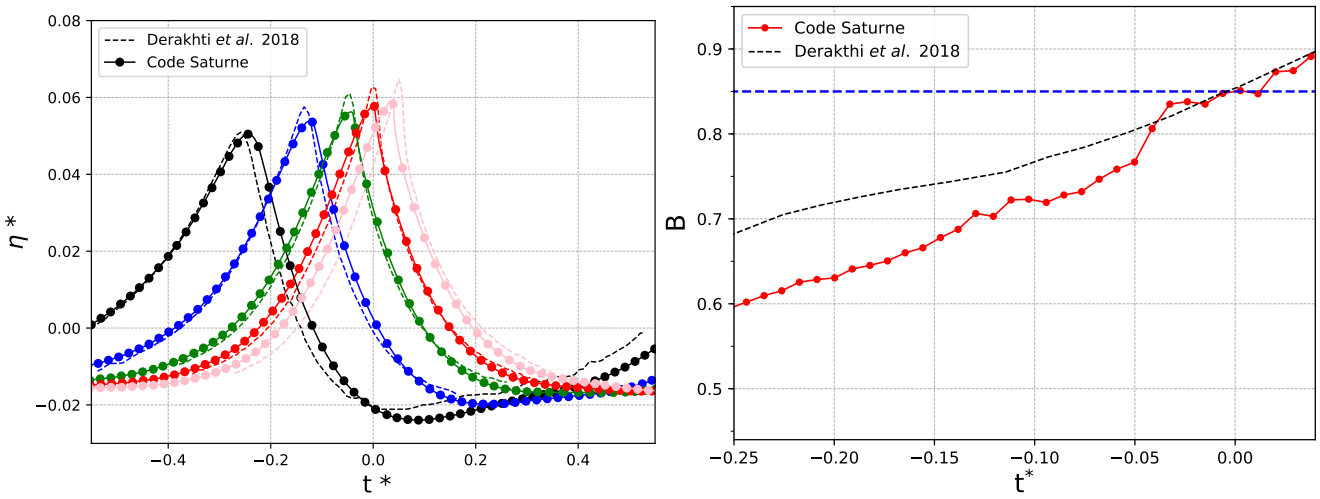

Fig. 3 Free surface elevation and breaking off set parameter evolution comparison between *Code_Saturne* and the numerical work from Derakhti et al. (2018). These results correspond to the spilling case A4. $\eta^* = (\eta - h)/L_c$ and $t^* = (t - t_{ob})/T_c$ with L_c, T_c being the wave length and period of the central frequency respectively and t_{ob} the time when $B = 0.85$.

a smooth surface this would be 2π), $\mathbf{n}$ the outwards normal vector to the boundary at point $\mathbf{x}$ and G the 2D free space Green's function of Laplace's equation. Fig. 2 presents the free-surface elevation ($\alpha = 0.5$) at a point 8 m from the generation boundary for both models. The initial wave appears to propagate quite similarly, though there is a slight decrease of energy towards the end of the wave packet.

Continuing this validation process, the results presented by Derakhti et al. (2018) are compared with the present model in Fig. 3. The free-surface location at different instants presents a fairly good match between *Code_Saturne* and previous numerical results. While the wave crests are slightly lower for the present model (compared to the FNPF solution) and there is an apparent time-shifting, the latter may be explained by the selection of these instants based on the location of the breaking point, which is defined using the breaking onset parameter $B = u_c/C$ defined as the ratio of the fluid velocity at the crest and the horizontal velocity of the crest. Barthelemy et al. (2018) reported that a value of $B = 0.85$ provides a threshold for breaking onset for 2D wave packets propagating in deep or intermediate uniform water depths. The evolution of this parameter is also presented in Fig. 3 and presents a similar slope, especially around the breaking threshold, with the results from Derakhti et al. (2018). The uneven evolution of the present model results comes from the difficulty of defining the wave crest location when its resembles an almost horizontal plane, see Fig. 4. Further grid refinements may provide improvements to the calculated wave celerity.

This section presented the results for different 2D breaking waves using *Code_Saturne*. Validation of the model is next carried out for different aspects of the process providing optimistic results to move towards more complex scenarios.

3D WAVE IMPACT ON A CYLINDER

This section presents a three-dimensional (3D) configuration using the same wave parameters from Derakhti et al. (2018) studied before. In this case, we consider a strong plunging, case A6, impacting on a vertical cylinder. Fig. 5 presents a detail of the mesh employed and the geometry. In order to reduce the computation costs, only half of the domain in the transverse direction is modelled, introducing a symmetric boundary condition for the central plane. All the other boundaries are

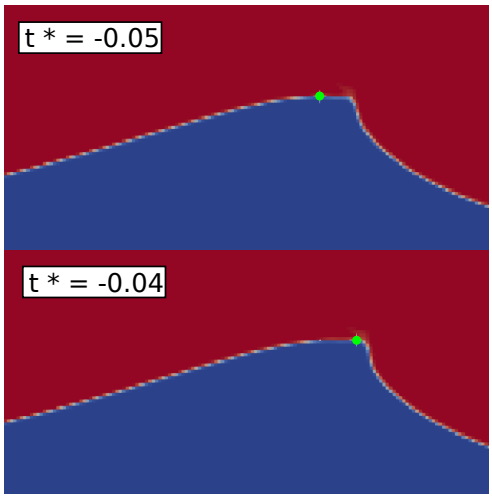

Fig. 4 Detected Wave crest location for two instances before the overturning for case A4, showing difficulties in tracking the crest.

maintained as in the 2D configuration.

The mesh is an extrusion of the 2D mesh from the previous section, with larger cell lengths ($\Delta x = \Delta y = \Delta z = 10$ mm) within the free surface region to reduce the computational costs. A cylinder of $R = 10$ cm is located close to the breaking location 7.46 m away from the generation boundary. The domain length in the transverse direction is $L_y = 40$ cm.

Fig. 6 presents the normalized horizontal total force on the cylinder exerted by the fluid during the breaking process. The black dots are the instants represented in Fig. 7 where the liquid velocity fields are presented. Initially, the quasi-static loads are dominant when the wave is approaching the structure, and these may be well predicted using Morison's formula. Next, a sudden increase in the force-time derivative occurs when the wave impacts the cylinder leading to the characteristic slamming effect and a maximum force is observed near $1.45\,\rho g D^3$. During this process, the fluid is rapidly decelerated as the water is forced to

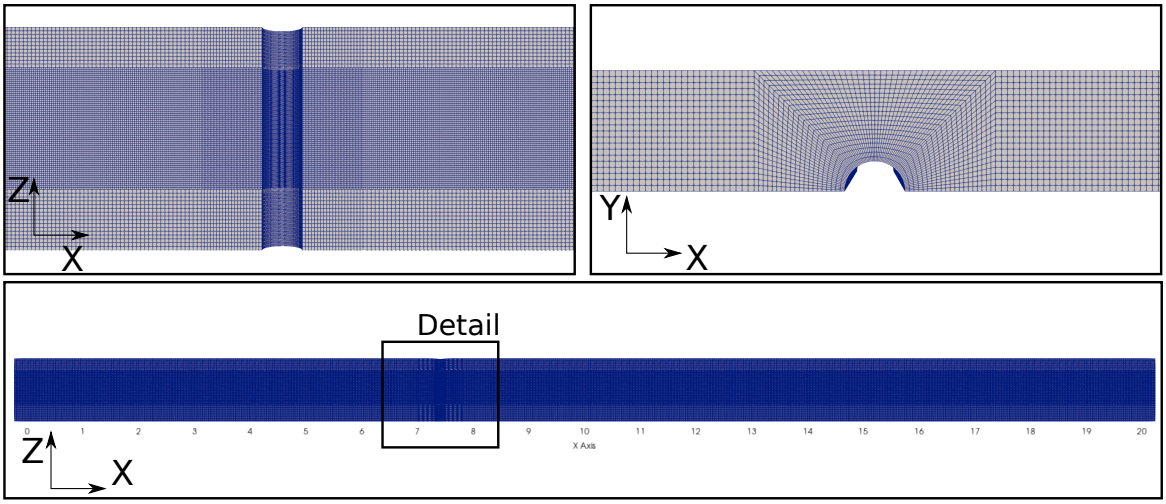

Fig. 5 Detail of the three-dimensional mesh used in slamming simulations.

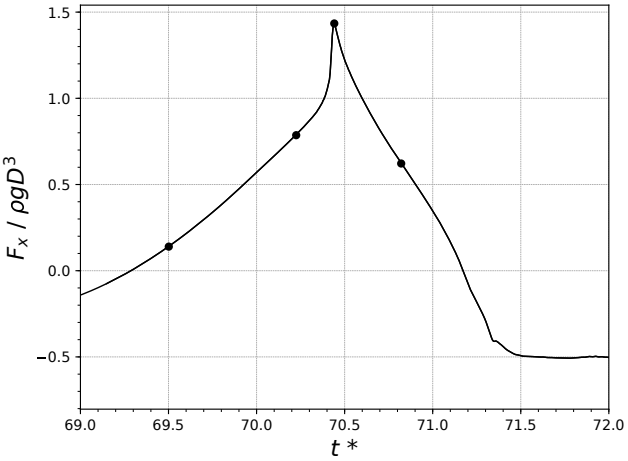

Fig. 6 Horizontal force of a focused wave strong plunging impact, case A6, on the cylinder obtained with *Code_Saturne*. The non-dimensional time is defined as $t^* = t\sqrt{g/h}$.

avoid the obstacle, producing a run-up visible at $t^* = 70.4$ and 70.8. This simulation lasted for 18 s of physical time until the impact occurs, the domain had 5.6 million cells and a fixed time step of 0.001 s was employed. Using 3 nodes, or 105 cores, from the high-performance computing cluster, Gaia (EDF), the computation finished after 10.5h.

CONCLUSIONS AND DISCUSSION

This paper presents the preliminary results obtained using the computational fluid dynamics solver, *Code_Saturne*, for modelling the wave breaking slamming on a cylinder phenomenon. The generation and propagation of phase-focused waves are analysed and validated against other numerical codes. It is shown the possibility to reproduce different wave breaking situation with fairly accurate reproduction of the overturning kinematics based on the breaking onset parameter evolution. A 3D computation of a breaking wave impact on a cylinder and the computational costs related are presented, providing optimistic results for proceeding now into a complete validation. More detailed comparisons, including studies of different engineering formulas for the slamming forces, will be presented at the conference.

ACKNOWLEDGEMENTS

This work is performed under financial support of grant ANR-10-IEED-0006-34, France Energies Marines project DIMPACT (Dimensionnement d'éoliennes flottantes prenant en compte les impacts de la raideur et du déferlement des vagues).

The authors would also like to thank Martin Ferrand for his helpful comments regarding *Code_Saturne*.

REFERENCES

Archambeau, F, Mechitoua, N and Sakiz, M (2004). "Code saturne: a finite volume code for the computation of turbulent incompressible flows- industrial applications", *International Journal on Finite Volumes*, 1, 1-62.

Barthelemy, X, Banner, M. L, Peirson, W. L, Fedele, F, Allis, M and Dias, F (2018). "On a unified breaking onset threshold for gravity waves in deep and intermediate depth water ", *Journal of Fluid Mechanics*, 841, 463–488.

Corte, C and Grilli, S (2006). "Numerical Modeling of Extreme Wave Slamming on Cylindrical Offshore Support Structures ", *Proc. 16th Offshore and Polar Engng. Conf.*, 394-401.

Dean, R. G, and Dalrymple, R. A (1991). "Water wave mechanics for engineers and scientists ", *World Scientific*.

Derakhti, M, Banner, M. L, and Kirby, J. T (2018). "Predicting the breaking strength of gravity water waves in deep and intermediate depth ", *Journal of Fluid Mechanics*, 848.

Ferrand, M and Harris, J (2021). "Finite volume arbitrary Lagrangian-Eulerian schemes using dual meshes for ocean wave applications ", *Computers and Fluids*, 219, 104860.

Filipot, J.-F, Guimaraes, P, Leckler, F, Hortsmann, J, Carrasco, R, Leroy, E, Fady, N, Accensi, M, Prevosto, M, Duarte, R, Roeber, V, Benetazzo, A, Raoult, C, Franzetti, M, Varing, A and Le Dantec, N (2019). "La Jument lighthouse: a real-scale laboratory for the study of giant waves and their loading on marine structures", *Philosophical Transactions of the Royal Society A: Mathematical, Physical and Engineering Sciences*, 377, 20190008.

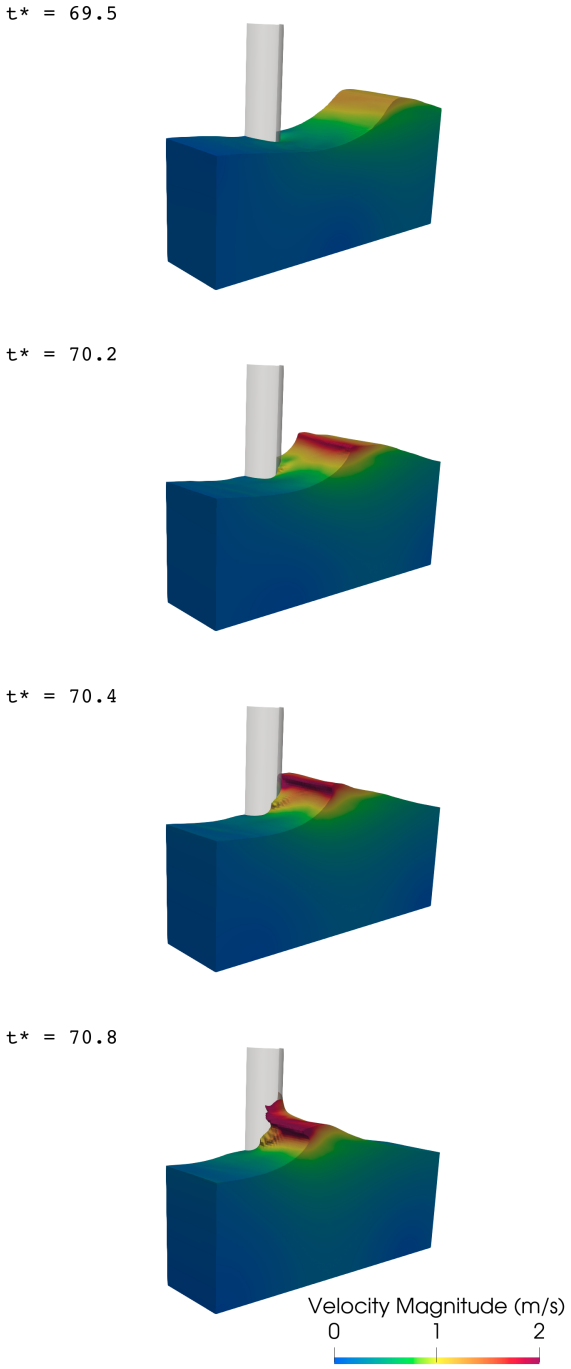

Fig. 7 Velocity fields at four relevant instants (see Fig. 6) during a focused wave strong plunging impact on a cylinder.

Goda, Y, Haranaka, S and Kitahata, M (1966). "Study of impulsive breaking wave forces on piles ", *PARI Report*, 005-06.

Grilli, S. T, Skourup, J and Svendsen, I. A (1989). "An efficient boundary element method for nonlinear water waves ", *Engineering Analysis with Boundary Elements*, 6, 97-107.

Grilli, S. T and Subramanya, R (1996). "Numerical modeling of wave breaking induced by fixed or moving boundaries ", *Computational Mechanics*, 17, 374-391.

Morison, J, Johnson, J and Schaaf, S (1950). "The Force Exerted by Surface Waves on Piles ", *Journal of Petroleum Technology*, 2, 149-154.

Paulsen, B. T, de Sonneville, B, van der Meulen, M and Jacobsen, N. G (2019). "Probability of wave slamming and the magnitude of slamming loads on offshore wind turbine foundations ", *Coastal Engineering*, 143, 76-95.

Pierella, F, Lindberg, O, Bredmose, H, Bingham, H, Read, R. W and Engsig-Karup, A. P (2020). "The DeRisk database: extreme design waves for offshore wind turbines ", *Marine Structures*, 46.

Ransley, E, Yan, S, Brown, S, Hann, M, Graham, D, Windt, C, Schmitt, P, Davidson, J, Ringwood, J, Musiedlak, P.-H, Wang, J, Wang, J, Ma, Q, Xie, Z, Zhang, N, Zheng, X, Giorgi, G, Chen, H, Lin, Z, Qian, L, Ma, Z, Bai, W, Chen, Q, Zang, J, Ding, H, Cheng, L, Zheng, J, Gu, H, Gong, X, Liu, Z, Zhuang, Y, Wan, D, Bingham, H and Greaves, D (2020). "A blind comparative study of focused wave interactiosn with floating structures (CCP-WSI Blind Test Series 3) ", *International Journal of Offshore and Polar Engineering*, 30, 1-10.

Rapp, R. J, Melville, W. K and Longuet-Higgins, M. S (1990). "Laboratory measurements of deep-water breaking waves ", *Philosophical Transactions of the Royal Society of London. Series A, Mathematical and Physical Sciences*, 331, 735-800.

Saincher, S, Sriram, V, Agarwal, S and Schlurmann, T (2022). "Experimental investigation of hydrodynamic loading induced by regular, steep non-breaking and breaking focused waves on a moving cylinder", *European Journal of Mechanics - B/Fluids*.

Sriram, V, Agarwal, S and Schlurmann, T (2020). "Laboratory study on steep wave interaction with fixed and moving cylinder ", *Proc. 30th International Ocean and Polar Engineering Conference*, 2221.

Sriram, V, Schlurmann, T and Schimmels, S (2015). "Focused wave evolution using linear and second order wavemaker theory ", *Applied Ocean Research*, 53, 279-296.

Tromans, P, Anaturk, A and Hagemeijer, P (1991). "A new model for the kinematics of large ocean waves-application as a design wave ", *Proc. 1st International Conference on Ocean, Offshore and Arctic Engineering*, 15 pp.

Veic, D and Suilisz, W (2018). "Impact pressure distribution on a monopile structure excited by irregular breaking wave ", *Polish Maritime Research*, 25:29-35.

von Karman, T (1929). "The Impact on Seaplane Floats during Landing ", *National Advisory Committee for Aeronautics Technical*.

Vyzikas, T, Stagonas, D, Maisondieu, C and Greaves, D (2021). "Intercomparison of three open-source numerical flumes for the surface dynamics of steep focused wave groups ", *Fluids*, 6:28 pp.

Wagner, H (1932). "Phenomena associated with impacts and sliding on liquid surface ", *ZAMM - Journal of Applied Mathematics and Mechanics / Zeitschrift für Angewandte Mathematik und Mechanik*, 12:193-215.

Wienke, J and Oumeraci, H (2005). "Breaking wave impact force on a vertical and inclined slender pile—theoretical and large-scale model investigations", *Coastal Engineering*, 52(5):435-462.

Zhang, D, Jiang, C, Liang, D, Chen, Z, Yang, Y and Shi, Y (2014). "A refined volume-of-fluid algorithm for capturing sharp fluid interfaces on arbitrary meshes ", *Journal of Computational Physics*, 274:709-736.